

## Two-fluid simulations of magnetic reconnection during merging-compression start-up in the MAST Spherical Tokamak

A. Stanier<sup>1</sup>, P. Browning<sup>1</sup>, M. Gordovskyy<sup>1</sup>,

K. G. McClements<sup>2</sup>, M. P. Gryaznevich<sup>2,3</sup>, V. S. Lukin<sup>4</sup>

<sup>1</sup> *Jodrell Bank Centre for Astrophysics, University of Manchester, Manchester M13 9PL, UK*

<sup>2</sup> *EURATOM/CCFE Fusion Association, Culham Science Centre, Abingdon OX14 3DB, UK*

<sup>3</sup> *Present affiliation: Imperial College of Science and Technology, London SW7 2AZ, UK*

<sup>4</sup> *Space Science Division, Naval Research Laboratory, Washington DC 20375, USA*

In a highly conducting plasma, the magnetic field is frozen-in to the bulk electron flow. However, if there exists a finite electric field parallel to the magnetic field, then magnetic reconnection can change field-line connectivity towards a state of lower magnetic energy. Reconnection is a plausible explanation for intense heating and particle acceleration in solar flares and in the magnetotail of Earth [1]. In a magnetic confinement fusion device, reconnection can create magnetic islands, leading to a local flattening of pressure profiles and a degradation in plasma confinement. Studying magnetic reconnection in a controlled experimental setting can give valuable insights into this fundamental plasma process.

We study the merging-compression method of plasma start-up in the Mega-Ampere Spherical Tokamak (MAST) as a magnetic reconnection experiment. Here, two toroidal flux-ropes with parallel currents are produced around in-vessel poloidal field coils. These flux-ropes are mutually attracted and merge at the mid-plane of the vessel through reconnection of the poloidal field. The plasma forms Spherical Tokamak (ST) configurations with plasma currents of up to 0.5 MA, and with temperatures reaching 1 keV on millisecond timescales through extremely rapid reconnection heating. In comparison with other dedicated reconnection experiments MAST has strong toroidal and poloidal magnetic fields,  $\mathbf{B}_T \sim 0.5$  T and  $\mathbf{B}_p > 0.1$  T, making it the highest Lundquist number,  $S \sim 10^4 - 10^7$ , and lowest plasma beta,  $\beta \sim 10^{-4} - 10^{-2}$ , reconnection experiment currently in operation [2]. Also, the high-resolution Thomson Scattering (TS) diagnostic gives detailed profiles of electron temperature and density which are essential for understanding the reconnection process.

Here we present results from non-linear two-dimensional fluid simulations of merging start-up on MAST. We study the effects of tight-aspect ratio toroidal geometry and two-fluid physics on the reconnection, and draw comparisons with experimental data.

We solve the compressible Hall-MHD equations in normalised form (see [3] for a full derivation) using the 2D HiFi [4, 5] spectral-element framework. The variables evolved are nor-

malised by MAST start-up plasma values: density  $n_0 = 5 \times 10^{18} \text{ m}^{-3}$ , length-scale  $L_0 = 1 \text{ m}$ , magnetic field  $B_0 = 0.5 \text{ T}$ , and temperature  $T_0 = T_{e,0} = T_{i,0} = 10 \text{ eV}$ . Velocities are normalised by the Alfvén speed  $v_0 = B_0(\mu_0 n_0 m_i)^{-1/2}$ , the electric field by  $E_0 = v_0 B_0$ , and pressures by  $p_0 = B_0^2/2\mu_0$ . The full set of equations is

$$\partial_t n + \nabla \cdot (n \mathbf{v}_i) = 0 \quad (1)$$

$$\partial_t (n \mathbf{v}_i) + \nabla \cdot (n \mathbf{v}_i \mathbf{v}_i + p \mathbb{I} + \boldsymbol{\pi}_i) = \mathbf{j} \times \mathbf{B} \quad (2)$$

$$\mathbf{E} = -\partial_t \mathbf{A} = -\mathbf{v}_e \times \mathbf{B} - \frac{d_i}{n} \nabla p_e + \eta \mathbf{j} - \eta_H \nabla^2 \mathbf{j} \quad (3)$$

$$\partial_t \mathbf{B} = -\nabla \times \mathbf{E} \quad (4)$$

$$(\gamma - 1)^{-1} [\partial_t p + \mathbf{v}_i \cdot \nabla p + \gamma p \nabla \cdot \mathbf{v}_i] = \eta j^2 + \eta_H (\nabla \mathbf{j})^2 - \boldsymbol{\pi}_i : \nabla \mathbf{v}_i - \nabla \cdot \mathbf{q} \quad (5)$$

where  $n$  is the density,  $\mathbf{v}_i$  and  $\mathbf{v}_e$  the ion and electron velocities ( $\mathbf{v}_e = \mathbf{v}_i - d_i \mathbf{j}/n$ ),  $\mathbf{B}$  the magnetic field,  $p = p_i + p_e$  the total (sum of the ion and electron) thermal pressure,  $\mathbf{j} = \nabla \times \mathbf{B}$  the current density,  $\mathbf{E}$  the electric field and  $\mathbf{A}$  the magnetic vector potential. The ion stress tensor is  $\boldsymbol{\pi}_i = -\mu(\nabla \mathbf{v}_i + \nabla \mathbf{v}_i^T)$ , and the heat-flux vector  $\mathbf{q}$  has anisotropic form  $\mathbf{q} = -\kappa_e^{\parallel} \nabla_{\parallel} T - \kappa_i^{\perp} \nabla_{\perp} T$  where  $\nabla_{\parallel} = \hat{\mathbf{b}}(\hat{\mathbf{b}} \cdot \nabla)$ . The coefficients are the normalised ion-skin depth,  $d_i = c(n_0 e^2 / \epsilon_0 m_i)^{-1/2} L_0^{-1} = 0.145$ , the resistivity  $\eta = (\mu_0 v_0 L_0)^{-1} \eta_{Sp,\parallel} = 10^{-5}$  based on the parallel Spitzer value, hyper-resistivity  $\eta_H$ , viscosity  $\mu = (\mu_0 v_0 L_0)^{-1} \mu_i^{\parallel} = 10^{-3}$  based on the parallel value but treated as a free parameter, and the parallel electron,  $\kappa_e^{\parallel}$ , and perpendicular ion,  $\kappa_i^{\perp}$ , heat conductivities. The final term in equation (3) is the hyper-resistivity [3], or anomalous electron viscosity. It is used to set the scale for the electron diffusion region, and a dissipation scale for waves with quadratic dispersion. In this study we vary  $\eta$ ,  $\mu$  and  $\eta_H$  to study the scaling effects of collisions on the merging.

Resistive MHD studies ( $d_i = 0$ ) and Hall-MHD studies ( $d_i = 0.145 \text{ m}$ ) in Cartesian geometry are described in [6], here we present results from a toroidal  $(R, \phi, Z)$  Hall-MHD simulation. The initial flux-ropes are modelled as localised distributions of parallel toroidal current  $j_{\phi}$ , see the first panel in Figure 1. The flux-ropes are balanced against the pinch-force by a paramagnetic increase in the toroidal field (due to the low poloidal beta  $\beta_p = 2 \times 10^{-3} \ll 1$ ). Outside of the flux-ropes the toroidal field has the vacuum radial dependence  $B_{\phi,0} = -B_0 R_0 / R$ , where  $R_0 = 0.85 \text{ (m)}$  is the major radius. The dashed line is the fieldline that coincides with the magnetic separator at  $t = 0$ . This separates the “private flux”, which is available for reconnection, from the “public flux”, which surrounds both flux-ropes and includes line-tied vertical flux balancing a radially outwards hoop force. The boundaries are conducting wall, perfect slip and zero normal temperature gradient, with the additional line-tying condition on the  $Z = \pm 2.2$  boundaries.

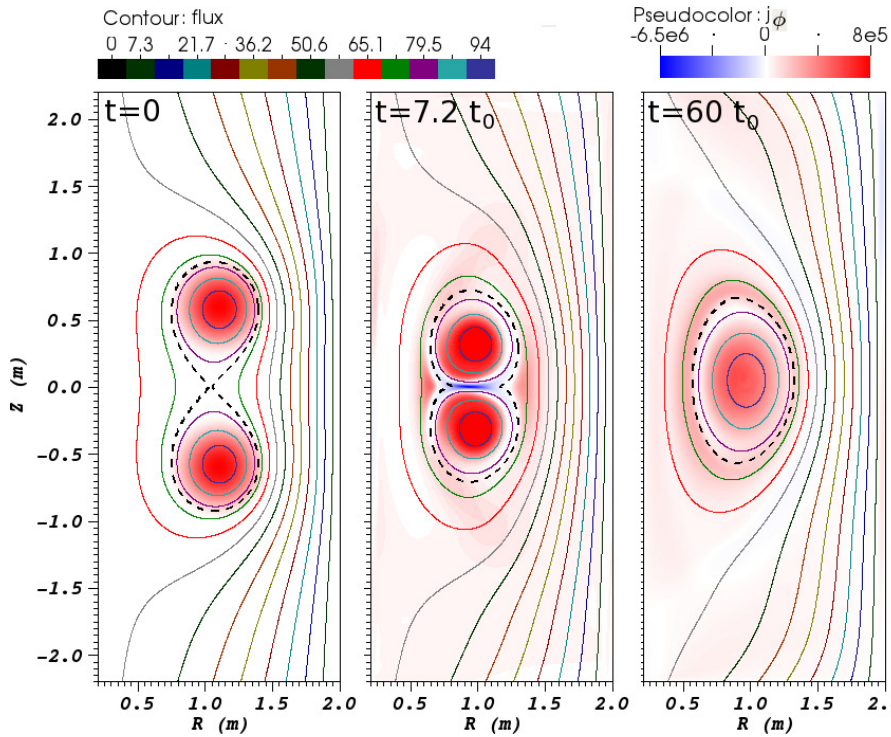


Figure 1: Toroidal current  $j_\phi$ , and flux contours  $\psi = RA_\phi$ , at three snapshots. The dashed fieldline coincides with the magnetic separator at  $t = 0$ .

The plasma density is shown in Figure 2 for a resistive MHD, and a Hall-MHD simulation in toroidal geometry when an equal amount of flux has been reconnected. In resistive MHD, the reconnection outflow jets into the small inboard volume cause order one density increases close to the central post, and there is a density cavity on the outboard side. In the Hall-MHD simulation parallel electron velocity gradients along newly reconnected fieldlines (see also [6, 7]) cause an additional “quadrupole” density pattern. The bottom panel shows simulated TS profiles of electron density. At  $t = 20t_0$  there is a double-peak in the density profile, but the outer peak is due to the quadrupole and disappears over time. These simulated density profiles agree well with the experimental TS data [2].

The middle panel shows the flux-rope after they have been mutually attracted towards the midplane and during reconnection. The X-point has collapsed to form a thin Current Sheet (CS) which has length comparable to the flux-rope radii. The final panel shows a single ST plasma, with nested flux-surfaces, after merging.

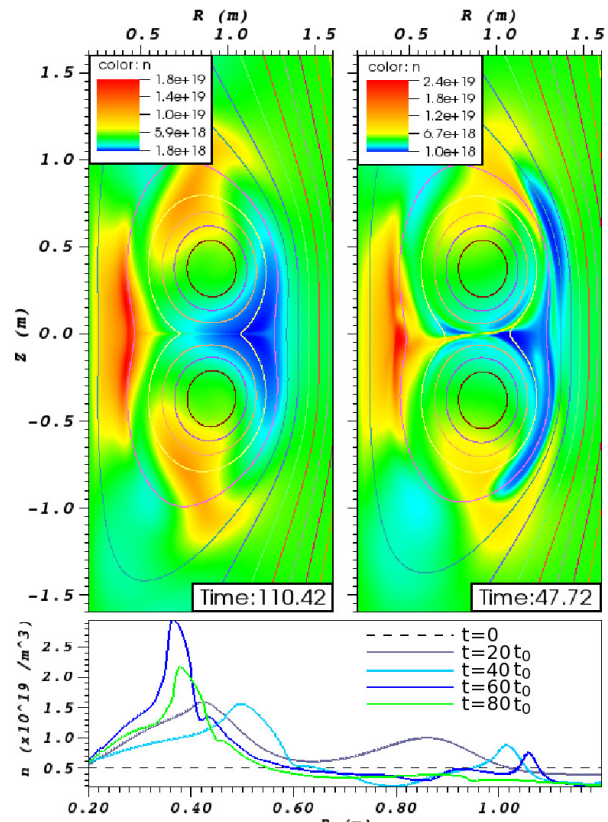


Figure 2: Above: Density (colour) for resistive MHD (left) and Hall-MHD (right) simulations. Below: Density profiles at midplane for Hall-MHD.

Figure 3 shows how varying collisionality, done here through the hyper-resistivity  $\eta_H$ , affects the CS. (Here we use Cartesian geometry ( $R, T, Z$ ), have uniform guide-field outside the flux-ropes,  $B_T = B_0$ , and no line-tied flux.) For the highest collision-rate,  $\eta_H = 10^{-6}$ , the CS is very low aspect-ratio and stable against fragmentation. For  $\eta_H = 10^{-8}$  the CS breaks up through a tearing-type instability, forming a large island that is not ejected, and stalls the reconnection, due to symmetries present in Cartesian geometry (in the toroidal simulations this symmetry is broken and the island is ejected [6]).

The final panel in Figure 3, with  $\eta_H = 10^{-10}$ , has a CS that spreads preferentially across the lower-left upper-right separator. The outflow channel opens up, resembling the classical picture of fast reconnection. This occurs when the CS width drops below the ion-sound radius  $\rho_{is} = \sqrt{T_e/m_i}/\Omega_{ci}$ , where  $\Omega_{ci}$  is the ion gyro-frequency. This CS geometry could explain a localised  $T_e$  peak seen in experiment [2], provided electron heating is co-spatial with current [6].

This work was funded by STFC, the US DoE Experimental Plasma Research program, the RCUK Energy Programme under grant EP/I501045, and by the European Communities under the Contract of Association between EURATOM and CCFE. The views and opinions expressed herein do not necessarily reflect those of the European Commission.

## References

- [1] E.G. Zweibel and M. Yamada, *Ann. Rev. Astron. Astrophys.*, **47**, 291 (2009)
- [2] Y. Ono, H. Tanabe, T. Yamada et al., *Plasma Phys. & Controlled Fusion*, **54**, 12 (2012)
- [3] D. Biskamp, *Magnetic Reconnection in Plasmas*, Cambridge University Press 2000
- [4] A.H. Glasser and X.Z. Tang, *Comp. Phys. Comm.*, **164**, 237 (2004)
- [5] V.S. Lukin, Ph.D. thesis, Princeton University, 2007
- [6] A. Stanier et al., *Phys. Plasmas*, in preparation, 2013
- [7] R.G. Kleva, J.F. Drake and F.L. Waelbroeck, *Phys. Plasmas*, **2**, 23 (1995)

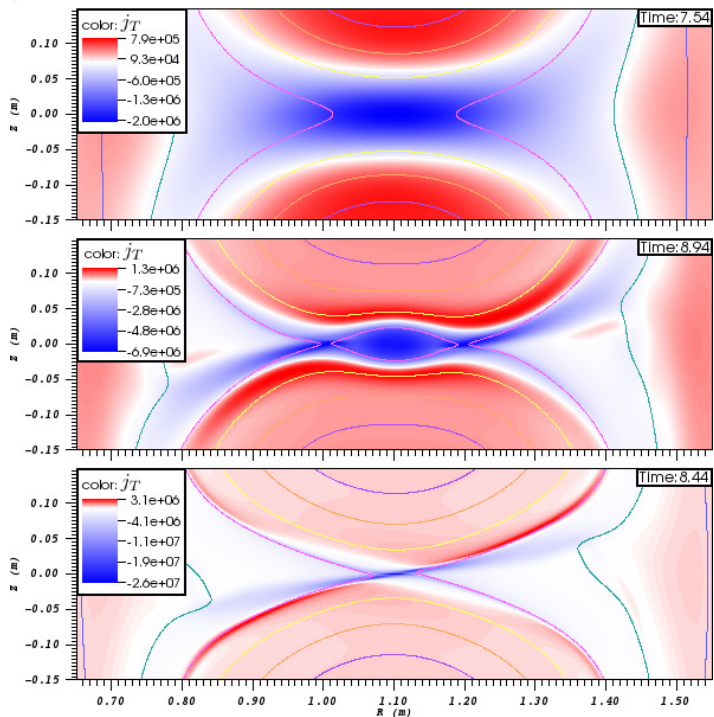


Figure 3: Current density  $j_T$  for infinite aspect-ratio simulation for  $\eta_H = 10^{-6}$  (top),  $10^{-8}$  (middle) and  $10^{-10}$  (bottom).